Finite-size effects at temperature-driven first-order transitions

Murty S. S. Challa and D. P. Landau
Center for Simulational Physics, University of Georgia, Athens, Georgia 30602

K. Binder
*Institute fur Physik, Universität Mainz, Postfach 3980, D-6500 Mainz, West Germany**
and Center for Simulational Physics, University of Georgia, Athens, Georgia 30602
(Received 18 February 1986)

We study the finite-size effects at a temperature-driven first-order transition by analyzing various moments of the energy distribution. The distribution function for the energy is approximated by the superposition of two weighted Gaussian functions yielding quantitative estimates for various quantities and scaling form for the specific heat. The rounding of the singularities and the shifts in the location of the specific-heat maximum are analyzed and the characteristic features of a first-order transition are identified. The predictions are tested on the ten-state Potts model in two dimensions by carrying out extensive Monte Carlo calculations. The results are found to be in good agreement with theory. Comparison is made with the second-order transitions in the two- and three-state Potts models.

I. INTRODUCTION

It is a well-established fact that the finite size of a system introduces systematic deviations from the macroscopic behavior at a second-order transition.[1–7] A knowledge of the finite-size effects is very useful because one can obtain the various thermodynamic quantities for small systems (using transfer matrix calculations, computer simulations, etc.) and then extrapolate to the infinite lattice in a nontrivial manner. However, finite-size effects at first-order transitions have begun to receive attention comparatively recently.[8–13] The difficulties are particularly acute in simulations where locating the transition point and diagnosing the order of the transition have been long-standing problems. Binder and Landau[12] (hereafter referred to as I) studied the case of a field-driven first-order transition (Ising model below the critical temperature) using a phenomenological theory and Monte Carlo simulations. This present work is a natural extension of I and we present here our studies of a temperature-driven first-order transition.

First-order transitions are characterized by discontinuities in the first derivatives of the free energy, e.g., the internal energy and the magnetization. This results in δ-function singularities in the specific heat and susceptibility at the transition. The system does not anticipate the transition and the correlation length remains finite when one approaches the transition, apart from systems where a continuous symmetry is broken[13] which are outside of consideration here. The singularities at a first-order transition are purely due to phase coexistence and there is no critical region and no critical exponents. At a second-order transition, on the other hand, the divergences are intimately linked to the divergence of the correlation length. While the susceptibility diverges, the specific heat may or may not diverge. (We henceforth confine this discussion to second-order transitions where the specific heat diverges with an exponent α.)

In a finite system the above divergences do not occur. Instead, *in both types of transitions,* one sees finite peaks in the specific heat and susceptibility near the transition point. Two effects appear because of finite lattice size: a "rounding" of the transition region occurs with the peak heights increasing with lattice size and the location of the maxima shift in a size-dependent fashion. In a second-order transition the rounding is due to the correlation length being limited by the lattice size, L, so that scaling theory predicts the specific-heat maximum to diverge as $L^{\alpha/\nu}$ and the half-width to decrease as $L^{-1/\nu}$ (Ref. 3). Note that we consider only systems with linear dimensions L_i finite in all spatial directions and of the same order and set $L_i = L$ for simplicity. At a first-order transition, L appears only because of the volume, L^d in d dimensions; thus, the maxima grow as L^d and the δ-function limit is obtained because the width decreases as L^{-d} (Refs. 8–13). Note that these specific predictions are reached only in the limit $L \to \infty$; moreover, there are usually errors in a Monte Carlo simulation which might render a more acceptable explanation of the divergences in terms of apparent exponents. Also, the discontinuities at a first-order transition are smeared out and there is no totally unambiguous way by which one can detect the order. The shifts in the locations of the peaks are not fully understood yet, though one might expect an L^{-d} dependence there also. Clearly, more quantitative estimates and analyses of other properties need to be made.

As a demonstration of the ambiguity which may be present we show the temperature dependence of the internal energy and order parameter for the ten-state Potts model in Fig. 1. (Details of the calculation will be given in Sec. III.) Without prior knowledge about this model it would clearly be quite difficult to locate the transition accurately or even to determine its order. We emphasize that these data are from very long Monte Carlo runs and

thus no hysteresis is seen (even though the transition is first order). The time dependence of the internal energy also shows very large fluctuations over different time scales and also does not unambiguously identify the order of the transition. This may be seen from Fig. 2 where the evolution of the internal energy is presented for both types of transitions. (Care must be taken in interpreting the figures for they depict the instantaneous values after every 5000 Monte Carlo steps. Consequently the short-time fluctuations have been omitted.)

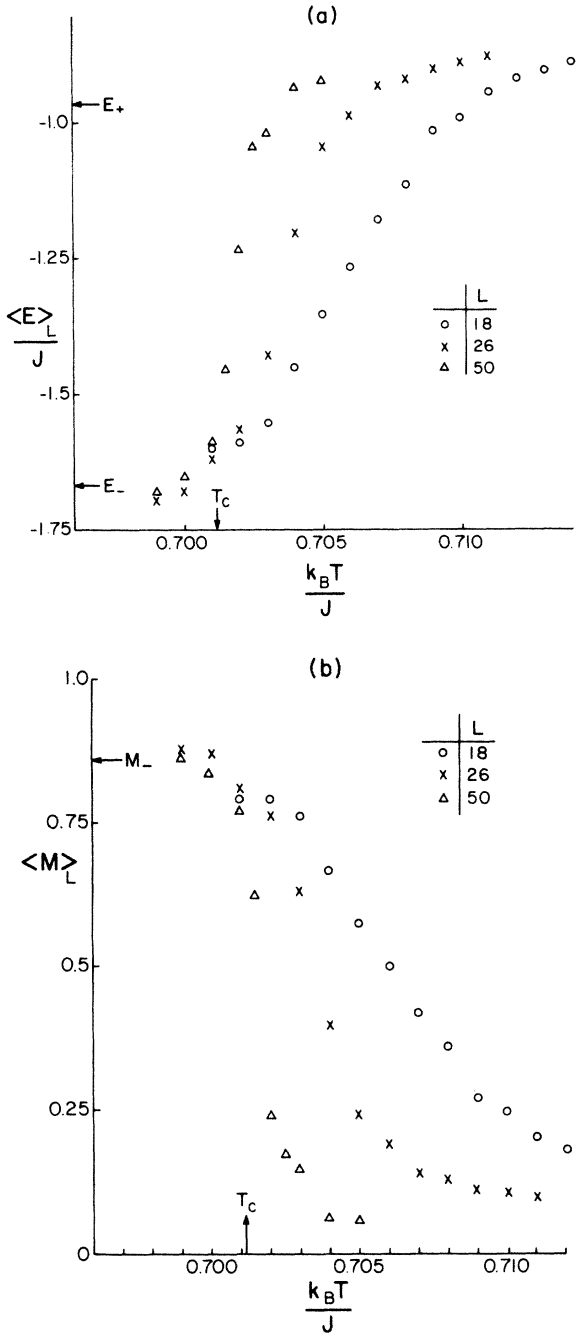

FIG. 1. Temperature dependence of the (a) internal energy and (b) order parameter for the ten-state Potts model. Characteristics of the first-order transition in the infinite lattice are indicated.

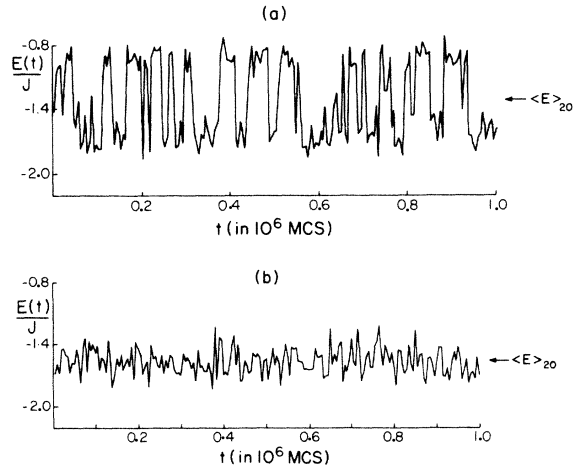

FIG. 2. Time dependence of the internal energy in Monte Carlo simulations on a 20×20 lattice. The instantaneous values of E are plotted after every 5000 Monte Carlo steps. (a) Fluctuations at the first-order transition in the ten-state Potts model. (b) Fluctuations at the second-order transition in the four-state Potts model.

Our approach to the problem is phenomenological and utilizes the theory of thermodynamic fluctuations.[14] The system is considered as a "black box" from which a value of E, the internal energy per site, is obtained at regular intervals (corresponding to the Monte Carlo passes). These values of E obey a probability distribution $P_L(E)$ and we assume that $P_L(E)$ is a Gaussian centered about the infinite-lattice energy E_0, characteristic of the temperature T, with a width proportional to the *infinite-lattice* specific heat C.[6,12] It can then be shown that

$$P_L(E)=\frac{A}{\sqrt{C}}\exp\left[-\frac{(E-E_0)^2L^d}{2k_BT^2C}\right],$$

where k_B is the Boltzmann constant and A is a normalization constant. [The treatment is parallel to that of I except that we consider here $P_L(E)$ instead of the magnetization distribution $P_L(s)$ of I.] We further argue that the distinctive feature of a first-order transition is phase coexistence so that at the transition point, $P_L(E)$ is a superposition of two Gaussians centered at E_+ and E_-. (E_+ and E_- are the internal energies at the transition in the high- and low-temperature phases, respectively.) Away from the transition, the Gaussians are centered at the energies characteristic of the temperature. The Gaussians are weighted by the Boltzmann factors of the respective free energies so that the double-Gaussian behavior persists in finite lattices over a small temperature range. Once $P_L(E)$ has been explicitly obtained, it is a trivial matter to calculate the quantities of interest, such as internal energy and specific heat, from suitable moments of $P_L(E)$. While the Gaussian approximation is justifiable for simulations of a single phase,[15] the double Gaussian would need correction terms for the region between the two

peaks. There, interface effects between domains of the various phases will play a major role[6] and significant deviations from Gaussian behavior may appear. We ignore the (unknown) corrections in order to have a tractable theory. In Fig. 3 we present some typical distributions obtained in the course of our simulations and one can see that the approximations we are making are reasonable.

The rest of the paper is organized as follows. The theory is presented in detail in Sec. II. In Sec. III the results of simulations of the two-dimensional ten-state Potts model are presented and comparison is made with the theoretical predictions.. Section IV summarizes our conclusions.

II. THEORY

In the following treatment all the quantities with the subscript + refer to the high-temperature phase and those with the subscript − refer to the low-temperature phase with T_c being the transition temperature. Thus, F_+, U_+, and S_+ are the free energy, internal energy, and entropy, respectively (all per spin), in the high-temperature phase. $E_+ = U_+(T_c)$ and $E_- = U_-(T_c)$ so that $E_+ - E_-$ is the latent heat. Since we are considering the system near T_c, we can assume that the specific heats, C_+ and C_-, do not vary with temperature. We consider only lattices that are larger than the correlation length of either phase so that all the quantities are the infinite lattice values. The measured quantities are labeled by the subscript L (the lattice size). Thus, $\langle E \rangle_L$, $\langle E^2 \rangle_L$, etc., are the moments of the energy distribution P_L on a hypercubic lattice of dimension d.

We stated earlier that $P_L(E)$ at the transition is a double Gaussian. If $\Delta T = T - T_c$, the Gaussians are centered at $E_+ + C_+ \Delta T$ and $E_- + C_- \Delta T$. Denoting $\Delta F = F_+ - F_-$, the weights for the Gaussians may be written in a symmetric form and we have

$$P_L(E) = A \left[\frac{a_+}{(C_+)^{1/2}} \exp\left[\frac{-[E-(E_+ + C_+ \Delta T)]^2 L^d}{2 k_B T^2 C_+} \right] + \frac{a_-}{(C_-)^{1/2}} \exp\left[\frac{-[E-(E_- + C_- \Delta T)]^2 L^d}{2 k_B T^2 C_-} \right] \right], \tag{1}$$

where $a_+ = [(C_+)^{1/2}] e^x$, $a_- = [(C_-)^{1/2}] q e^{-x}$, q (equal to 10 in our case) is the number of ordered states coexisting with the disordered state at T_c, and x is given by

$$x = \frac{-\Delta F L^d}{2 k_B T} \tag{2}$$

(d is the dimensionality). The question arises—How does one justify the above approximation? We do this by considering for the moment the space of the order-parameter components, which we denote by $\{\bar{\Psi}\}$ and recall from basic statistical mechanics that for $L \to \infty$ the probability distribution becomes

$$\tilde{P}_L(\bar{\Psi}) \propto \exp\left[\frac{-L^d F(\bar{\Psi})}{k_B T} \right], \tag{3}$$

where $F(\bar{\Psi})$ is the free-energy density of the system. Since the free energies of the disordered and ordered phases are equal at T_c, Eq. (3) implies that $\tilde{P}_L(\bar{\Psi})$ has $q+1$ peaks of equal height at T_c. If we consider only small deviations from the peak positions, i.e., relative deviations of $|\bar{\Psi}|$ from its peak positions of the order of $L^{-d/2}$, one may expand $F(\bar{\Psi})$ quadratically around each of these peaks of $\tilde{P}_L(\bar{\Psi})$ and thus replace each peak by a Gaussian. This is schematically illustrated in Fig. 4 for the simple case of a temperature-driven first-order transition in a Landau theory with a scalar order parameter Ψ:

$$F(\Psi) = F_0 + \frac{r}{2}\Psi^2 + \frac{u}{4}\Psi^4 + \frac{v}{6}\Psi^6 + \cdots, \tag{4}$$

where $F_0, r, u, v, \ldots$, are chosen such that $u < 0$, $v > 0$ (independent of temperature) and $r = r'(T - T_0)$. At T_c the free energy of the two ordered states ($\Psi = \pm M_{sp}$, where M_{sp} is the spontaneous magnetization) and the disordered state ($\Psi = 0$) are equal. If we expand $F(\Psi)$ quadratically around each of these minima as indicated by

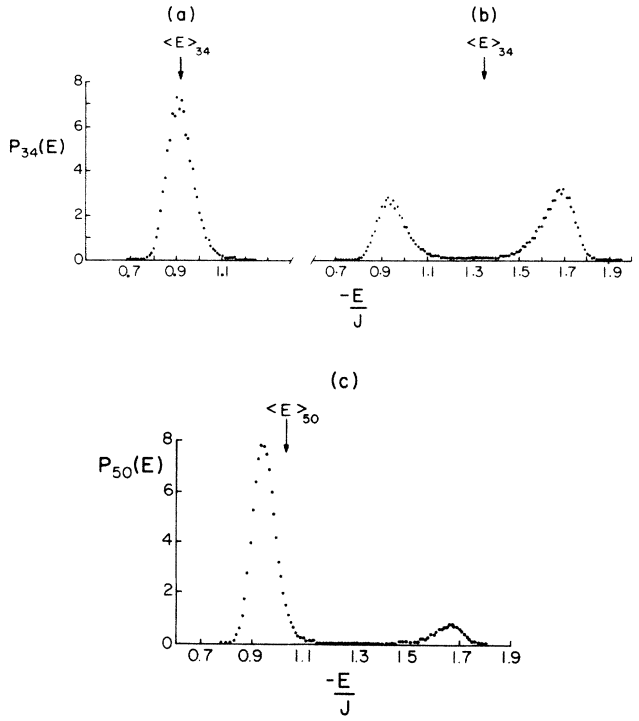

FIG. 3. Probability distributions of the internal energy at various temperatures obtained in simulations of the ten-state Potts model on $L \times L$ square lattices. The model has a first-order transition at $k_B T/J = 0.7012$. The specific-heat maxima are located at $k_B T/J = 0.7027$ for $L = 34$ and at 0.7018 for $L = 50$. The average values of the internal energies are also indicated. (a) Results from a single run of 4×10^6 Monte Carlo passes on a 34×34 lattice at a temperature far from the transition temperature. (b) Same as (a) except that T is very nearly equal to the transition temperature for $L = 34$. (c) Unequal distributions for a 50×50 lattice slightly away from the transition temperature. The number of Monte Carlo passes was 5×10^6.

the dashed curves in Fig. 4, $\tilde{P}_L(\Psi)$ becomes a sum of three Gaussian peaks, which have exactly equal height at T_c since then $F(\Psi=0)$ and $F(\Psi=\pm M_{sp})$ are exactly equal. Note that obviously nothing is implied about the "weights" of the Gaussian peaks (i.e., the area under the Gaussian distributions), which are controlled both by the free-energy minima and the curvature there (the curvatures at these minima in the case of Fig. 4 are controlled by the parameters $r,u,v,\ldots$, of the Landau expansion, and choosing enough terms in this expansion one can give them any value). Thus the remark made in I that in the general case the transition occurs when the Gaussian peaks have equal "weights" (i.e., areas) is in error, but as we shall see below, this is a valid definition of the effective transition temperature $T_c(L)$ in the finite system.

Since the order-parameter distribution contains (in the example of Fig. 4) three peaks of equal heights at T_c, the corresponding energy distribution must contain two peaks around $E=E_-$ and $E=E_+$, with $P_L(E_-)=2P_L(E_+)$ because both peaks $\tilde{P}_L(\Psi=+M_{sp})$ and $\tilde{P}_L(\Psi=-M_{sp})$ contribute to the same state with $E=E_-$, when one chooses the energy rather than the order parameter as the phase-space coordinate. Of course, this factor of 2 is specific to the Landau model, Eq. (4), which has a twofold-degenerate ordered phase; obviously if there is a

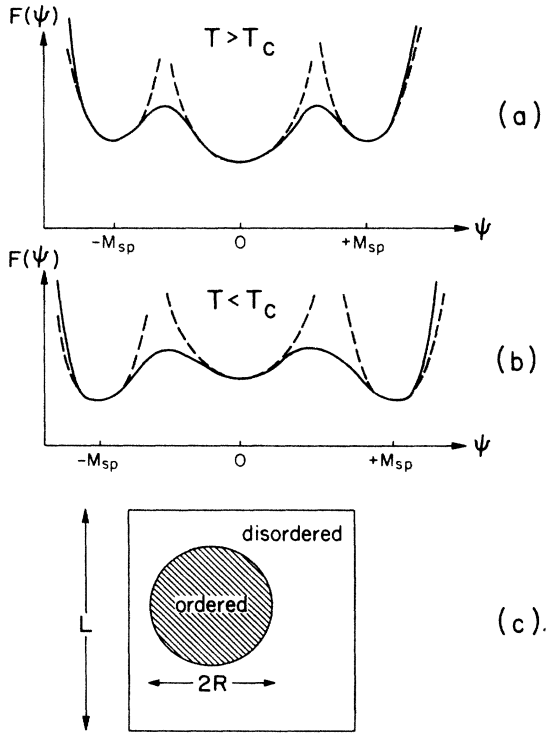

FIG. 4. Schematic variation of the free energy $F(\Psi)$ as given by Eq. (4) near a first-order transition occurring at $T_c=T_0+3u^2/(32r'v)$ in Landau theory (a) and (b). Note that the actual free energy for values of Ψ in the region between the minima is not given by Eq. (4) but rather is dominated by mixed-phase configurations as schematically sketched in (c). Dashed curves in (a) and (b) indicate the quadratic expansion around the minima which yields a triple-Gaussian approximation for $\tilde{P}_L(\Psi)$ in this case.

q-fold degeneracy we must have

$$P_L(E_-)=qP_L(E_+),\quad T=T_c\ , \tag{5}$$

and this is satisfied by Eq. (1) since $\Delta F=0$ at T_c.

Equation (1) is constructed such that it yields the correct first and second moments of the energy distribution, as will be shown in detail below; of course, higher-order reduced cumulants of the energy distribution are no longer described accurately. This already happens in the Landau theory: e.g., at $T\gg T_c$ in Fig. 4 there is only one minimum at $\Psi=0$, and in the quadratic expansion this implies that

$$U_L=1-\langle\Psi^4\rangle_L/3\langle\Psi^2\rangle_L^2\equiv 0\ .$$

In reality, due to the term of order Ψ^4 in Eq. (4) one must have a nonzero U_L (of order L^{-d}, cf. Ref. 6). Similarly, reduced cumulants of the energy distribution also are expected to have the order L^{-d} even if there is a single peak in $P_L(E)$. Apart from this failure to correctly describe the reduced cumulants of higher than second order, Eq. (1) is also seriously in error for states near the maxima of $F(\Psi)$ in Fig. 4. Equations (3) and (4) imply that $F_{max}(\Psi)-F_{min}(\Psi)$ is of order unity, and hence

$$P_L^{min}(E)/P_L^{max}(E)\propto\exp(-\text{const}\times L^d)\ .$$

But in reality states near the maxima of $F(\Psi)$ close to the thermodynamic limit are dominated by two-phase configurations [see Fig. 4(c)] which means that $F_{max}(\Psi)-F_{min}(\Psi)$ at T_c is of order $1/L$, due to the interface free-energy cost of the domain in Fig. 4(c). This implies that

$$P_L^{min}(E)/P_L^{max}(E)\propto\exp(-\text{const}L^{d-1})$$

for $T=T_c$. However, since even states near the central probability minimum have contributions which are exponentially smaller, this problem does not affect the low-order moments of $P_L(E)$. Of course, such states are crucial for understanding the dynamics of first-order transitions.[16]

We now discuss the energy and specific heat which follow from the postulate, Eq. (1). First, the constant A is obtained by the normalization condition,

$$\int_{-\infty}^{\infty}P_L(E)dE=1\ ,$$

so that

$$A=\left[\frac{L^d}{2\pi k_BT^2}\right]^{1/2}\frac{1}{a_++a_-}\ . \tag{6}$$

Then the first and second moments are easily found to be

$$\langle E\rangle_L=\frac{a_+E_++a_-E_-}{a_++a_-}+\frac{(a_+C_++a_-C_-)\Delta T}{a_++a_-}\ , \tag{7}$$

$$\langle E^2\rangle_L=\frac{a_+(E_++C_+\Delta T)^2+a_-(E_-+C_-\Delta T)^2}{a_++a_-}+\frac{k_BT^2}{L^d}\frac{(a_+C_++a_-C_-)}{a_++a_-}\ . \tag{8}$$

The fluctuation-dissipation theorem implies for the specific heat

$$C_L=\frac{L^d}{k_BT^2}(\langle E^2\rangle_L-\langle E\rangle_L^2)$$
$$=\frac{a_+C_++a_-C_-}{a_++a_-}$$
$$+\frac{a_+a_-L^d[(E_+-E_-)+(C_+-C_-)\Delta T]^2}{k_BT^2(a_++a_-)^2}\ . \tag{9}$$

Of course, alternatively the specific heat can also be obtained as the temperature derivative of the internal energy. From Eq. (7) we get

$$C_L=\frac{d\langle E\rangle_L}{dT}$$
$$=\frac{a_+C_++a_-C_-}{a_++a_-}$$
$$+2\frac{dx}{dT}\frac{a_+a_-[(E_+-E_-)+(C_+-C_-)\Delta T]}{(a_++a_-)^2}\ . \tag{10}$$

In the absence of external fields, $F_\pm=U_\pm-TS_\pm$ and $dF_\pm=-S_\pm dT$, and noting that $F_+(T_c)=F_-(T_c)$, we get

$$2\frac{dx}{dT}=\frac{L^d}{k_BT^2}(U_+-U_-)$$
$$=\frac{L^d}{k_BT^2}[(E_++C_+\Delta T)-(E_-+C_-\Delta T)]\ . \tag{11}$$

Using Eq. (11) in Eq. (10) we recover Eq. (9), and hence we have established the thermodynamic consistency of the ansatz, Eq. (1). (The generalization to the case when a magnetic field is present follows by noting that the magnetic Hamiltonian then represents the enthalpy and not the internal energy.) Note that Eq. (1) is much more general than the arguments drawn from Landau theory, which we have used as an illustration and motivation only.

We now approximate x in Eq. (2) by expanding F_+ and F_- about T_c up to $O(\Delta T)$. (Note that higher-order terms would involve the temperature variation of the specific heats C_+ and C_-.) Again using $F_+(T_c)=F_-(T_c)$, we obtain

$$\Delta F=\frac{-(E_+-E_-)\Delta T}{T_c}\ , \tag{12}$$

which yields

$$x=\frac{(E_+-E_-)\Delta TL^d}{2k_BTT_c}\approx\frac{(E_+-E_-)\Delta TL^d}{2k_BT_c^2}\ . \tag{13}$$

We now discuss the finite-size effects for the energy and specific heat which follow from Eqs. (7) and (9). For $\Delta T>0$ and $L\to\infty$, $a_+\to\infty$ and $a_-\to0$. If $\Delta T<0$, $a_+\to0$ and $a_-\to\infty$ in the same limit. Thus the internal energy behaves as

$$\langle E\rangle_L\to\begin{cases}E_++C_+\Delta T, & L\to\infty,\ T>T_c \text{ fixed}\ , \quad (14)\\ E_-+C_-\Delta T, & L\to\infty,\ T<T_c \text{ fixed}\ . \quad (15)\end{cases}$$

If we demand that $a_+=a_-=a$ we find

$$\langle E\rangle_L\approx\frac{E_++E_-}{2},\quad T=T_c(L)\ . \tag{16}$$

The condition $a_+=a_-$, which says that both states contribute to the integrated energy distribution with equal weight, can thus be taken as an effective $T_c(L)$ for the finite system, where the energy is just the arithmetic mean of the two states. From the definitions of a_+ and a_- and Eq. (13) we find

$$e^{2x}=q(C_-/C_+)^{1/2} \tag{17}$$

and

$$\frac{T_c(L)-T_c}{T_c}=\frac{k_BT_c\ln[q(C_-/C_+)^{1/2}]}{(E_+-E_-)L^d}\ . \tag{18}$$

As a result we conclude that there is a shift of T_c of order L^{-d}.

While Eqs. (14)–(18) refer to the limit where $L\to\infty$, we now consider the opposite limit $x\ll1$. We obtain, up to $O(\Delta T)$,

$$\langle E\rangle_L\approx\frac{E_+-E_-}{2}+\frac{(E_+-E_-)^2L^d[T-T_c(L)]}{4k_BT_c^2}\ . \tag{19}$$

This deviation from the infinite lattice behavior manifests itself in the smoothness of the $\langle E\rangle_L$ versus T curves (Fig. 1). We can obtain an order of magnitude estimate of the rounding by noting that the width of the transition region in a finite lattice corresponds to $x\sim1$. Thus

$$\frac{\Delta T_{\text{round}}}{T_c}\approx\frac{2k_BT_c}{(E_+-E_-)L^d}\ . \tag{20}$$

Equations (18) and (20) show that the rounding is the same order as the shift. Turning our attention to the specific heat, we see from Eq. (9) that

$$C_L\to C_+,\quad L\to\infty,\quad T>T_c \text{ fixed}\ , \tag{21}$$

$$C_L\to C_-,\quad L\to\infty,\quad T<T_c \text{ fixed}\ , \tag{22}$$

while the maximum value of C_L is [cf. also Eq. (19)]

$$C_L\mid_{\max}\approx\frac{C_++C_-}{2}+\frac{(E_+-E_-)^2L^d}{4k_BT_c^2}\ . \tag{23}$$

This result is found from noting that $C_L\mid_{\max}$ is found from $dC_L/dT=0$, which to leading order is identical to

$$\frac{d}{dT}(a_++a_-)=(a_+-a_-)\frac{dx}{dT}=0\ , \tag{24}$$

which again is solved by $a_+=a_-$, i.e., Eq. (18).

We have also considered the quantity V_L defined by

$$V_L=1-\frac{\langle E^4\rangle_L}{3\langle E^2\rangle_L^2}\ . \tag{25}$$

Although V_L does not have any obvious experimental significance, it is an extremely useful quantity in simulations[17] and behaves quite differently at first- and second-order transitions. We note that from Eq. (1)

$$\langle E^4\rangle_L=\frac{1}{a_++a_-}\left\{a_+\left[3\left[\frac{k_BT^2C_+}{L^d}\right]^2+\frac{6k_BT^2C_+}{L^d}(E_++C_+\Delta T)^2+(E_++C_+\Delta T)^4\right]\right.$$
$$\left.+a_-\left[3\left[\frac{k_BT^2C_-}{L^d}\right]^2+\frac{6k_BT^2C_-}{L^d}(E_-+C_-\Delta T)^2+(E_-+C_-\Delta T)^4\right]\right\}. \quad (26)$$

Although the expansion for V_L resulting from Eqs. (8), (25), and (26) is forbiddingly complicated and thus is not presented here, it is enough to examine V_L at $T_c(L)$ and far away from it. Away from the first-order transition, $P_L(E)$ is described by a single Gaussian so that, in the thermodynamic limit, the resulting δ-function singularity yields $\langle E^4\rangle=U_\pm^4$ and $\langle E^2\rangle=U_\pm^2$ ($U_\pm=E_\pm+C_\pm\Delta T$). Therefore

$$V_L=1-\frac{U_\pm^4}{3U_\pm^4}=\tfrac{2}{3},\quad L\to\infty,\quad T\neq T_c \text{ fixed}. \quad (27)$$

Equation (27), a trivial limit, is also true if the transition at T_c were second order and holds at T_c for the second-order transition as well [although the probability distribution $P_L(E)$ is essentially non-Gaussian, its relative width vanishes at T_c and in the thermodynamic limit $P_L(E)$ is a δ function as well]. When $P_L(E)$ is described by two Gaussians of equal weight, which happens at $T_c(L)$, we obtain a nontrivial limit

$$V_L\mid_{\min}=1-\frac{2(E_+^4+E_-^4)}{3(E_+^2+E_-^2)^2},\quad L\to\infty,\quad T=T_c(L). \quad (28a)$$

To leading order in L^{-d} we obtain

$$V_L\mid_{\min}=1-\frac{2(E_+^4+E_-^4)}{3(E_+^2+E_-^2)^2}-\frac{4k_BT_c^2}{L^d}\left[\frac{C_+E_+^2+C_-E_-^2}{(E_+^2+E_-^2)^2}-\frac{(C_++C_-)(E_+^4+E_-^4)}{3(E_+^2+E_-^2)^3}\right.$$
$$+\frac{2(E_+^3C_++E_-^3C_-)\ln[q(C_-/C_+)^{1/2}]}{3(E_+-E_-)(E_+^2+E_-^2)^2}$$
$$\left.-\frac{(E_+^4+E_-^4)(E_+C_++E_-C_-)\ln[q(C_-/C_+)^{1/2}]}{3(E_+-E_-)(E_+^2+E_-^2)^3}\right]. \quad (28b)$$

In the framework of the double-Gaussian approximation, the temperature T_L^v where this minimum of V_L occurs is identical to the temperature T_L^C where the specific-heat maximum occurs, and is given by Eq. (18). However, if we consider higher-order terms T_L^C and T_L^v are expected to differ by terms of order L^{-2d} and also $V_L\mid_{\min}$ has a correction term of order L^{-d}. Therefore it follows that a proper extrapolation of $V_L\mid_{\min}$ to the thermodynamic limit is also performed linearly in the variable L^{-d}. We emphasize that since Eq. (25) does not consider a reduced cumulant of the energy distribution, which would involve the odd moments as well, we are able to obtain the leading terms correctly, as given by Eqs. (27) and (28), entirely in terms of E_+ and E_-, and the quantity V_L is of order unity. The corrections to the Gaussian approximation, which are picked up by the reduced cumulant, appear in V_L as a finite-size correction only.

Finally we consider the case of an asymmetric field-driven transition (see I) where, in the thermodynamic limit at $h=H-H_c=0$, a first-order transition occurs with the magnetization M jumping from M_+ at $h=0^+$ to M_- at $h=0^-$. In terms of the susceptibilities χ_+ and χ_- at phase coexistence, the probability distribution of the order parameter becomes

$$P_L(s)=\frac{A}{(2\pi k_BT)^{1/2}}\left[\exp\left[-\frac{[(s-M_+)^2-2\chi_+sh]L^d}{2k_BT\chi_+}\right]+\exp\left[-\frac{[(s+M_-)^2-2\chi_-sh]L^d}{2k_BT\chi_-}\right]\right]$$

instead of Eq. (23) of I. Similarly, instead of Eq. (24) the normalization constant A becomes

$$A=L^{d/2}\left[\chi_+^{1/2}\exp\left[\frac{\chi_+h^2L^d}{2k_BT}\right]\exp\left[\frac{hM_+L^d}{k_BT}\right]+\chi_-^{1/2}\exp\left[\frac{\chi_-h^2L^d}{2k_BT}\right]\exp\left[\frac{-hM_-L^d}{k_BT}\right]\right]^{-1}.$$

Then

$$\langle s\rangle_L=AL^{-d/2}\left[(\chi_+h+M_+)\chi_+^{1/2}\exp\left[\frac{\chi_+h^2L^d}{2k_BT}\right]\exp\left[\frac{hM_+L^d}{k_BT}\right]\right.$$
$$\left.+(\chi_-h-M_-)\chi_-^{1/2}\exp\left[\frac{\chi_-h^2L^d}{2k_BT}\right]\exp\left[\frac{-hM_-L^d}{k_BT}\right]\right]$$

corrects Eq. (25) of I, and finally Eq. (26) of I should be replaced by

$$\langle s^2\rangle_L = AL^{-d/2}\left[\left[(\chi_+ h + M_+)^2 + \frac{k_B T\chi_+}{L^d}\right]\chi_+^{1/2}\exp\left[\frac{\chi_+ h^2 L^d}{2k_B T}\right]\exp\left[\frac{hM_+ L^d}{k_B T}\right]\right.$$
$$\left. + \left[(\chi_- h - M_-)^2 + \frac{k_B T\chi_-}{L^d}\right]\chi_-^{1/2}\exp\left[\frac{\chi_- h^2 L^d}{2k_B T}\right]\exp\left[\frac{-hM_- L^d}{k_B T}\right]\right] .$$

The expansions given here again express the principle that at the transition field H_c the peak heights of $P_L(s)$ have to be equal; the effective (shifted) transition field $H_c(L)$ occurs when the peak weights (areas) are effectively equal, i.e., for

$$h_c = H_c(L) - H_c = \frac{\ln(\chi_-/\chi_+)k_B T}{2(M_+ + M_-)L^d} .$$

Of course, in the symmetric case (where $M_+ = M_- = M$, $\chi_+ = \chi_-$) there is also no shift of $H_c = 0$ in this case as required by symmetry.

III. RESULTS FROM MONTE CARLO SIMULATIONS

We tested the theory by performing Monte Carlo simulations[18] of the ten-state Potts model on $L \times L$ square lattices with periodic boundary conditions. In a q-state Potts model the spin at the ith site, σ_i, can take on one of q different values, say, the numbers 1 to q. ($q = 10$ for our system.) The Hamiltonian is given by

$$H = -J\sum_{(i,j)} \delta_{\sigma_i \sigma_j} , \tag{29}$$

where δ is the Kronecker delta, J is the interaction strength (>0 for the ferromagnetic case) and the sum runs over all the nearest-neighbor pairs.

The Potts model is a generalization of the Ising model and has been extensively studied.[19–21] The properties of the model are q dependent and Baxter[20] has shown that in two dimensions, the model has a second-order transition for $q \leq 4$ and a first-order transition for $q > 4$. Baxter's results for T_c and the latent heat are the following:

$$\frac{k_B T_c}{J} = [\ln(1+\sqrt{q})]^{-1} , \tag{30}$$

$$\frac{E_+ - E_-}{J} = 2(1+\sqrt{q})\tanh\frac{\theta}{2}\prod_{n=1}^{\infty}[\tanh(n\theta)]^2 , \tag{31}$$

where $2\cosh\theta = \sqrt{q}$. We can obtain E_+ and E_- by using the above with the results of Kihara *et al.*:[21]

$$\frac{E_+ + E_-}{2J} = -\left[1 + \frac{1}{\sqrt{q}}\right] . \tag{32}$$

The order parameter, m, is defined as follows. Let N_1 be the number of spins in state 1, N_2 be the number in state 2, etc., and $N_{\max} = \max(N_1, N_2, \ldots, N_q)$. Then

$$m = \frac{q(N_{\max}/N) - 1}{q - 1} . \tag{33}$$

Kim[22] has given a large-q expansion for the discontinuity, Δm, in two dimensions (confirmed later by Baxter[23] who has given an exact expression for Δm). The result is

$$\Delta m = 1 - q^{-1} - 3q^{-2} - 9q^{-3} - 27q^{-4} - \cdots . \tag{34}$$

We see from the above exact results that the $q = 10$ model has a prominant first-order transition with $T_c = 0.701\,232$, $E_+ = -0.9682$, $E_- = -1.6643$, $m_- = 0.8572$, and $m_+ = 0$. (It is to be understood henceforth that the units for the temperature are J/k_B and those for the energy are J.)

The simulations were done using standard Monte Carlo techniques on lattices of sizes $L = 18$ to 50. The strong first-order character of the transition introduces pronounced metastabilities with the system spending most of the time in one of the two phases and very large run times are required to sample the distribution effectively. For the larger lattices up to 35×10^6 Monte Carlo steps (MCS)/site were needed per data point and for the smaller lattices up to 8×10^6 MCS were sufficient. The data points are averages over several different runs of 4 to 6×10^6 MCS each and represent different starting configurations, random number sequences, etc. The calculations

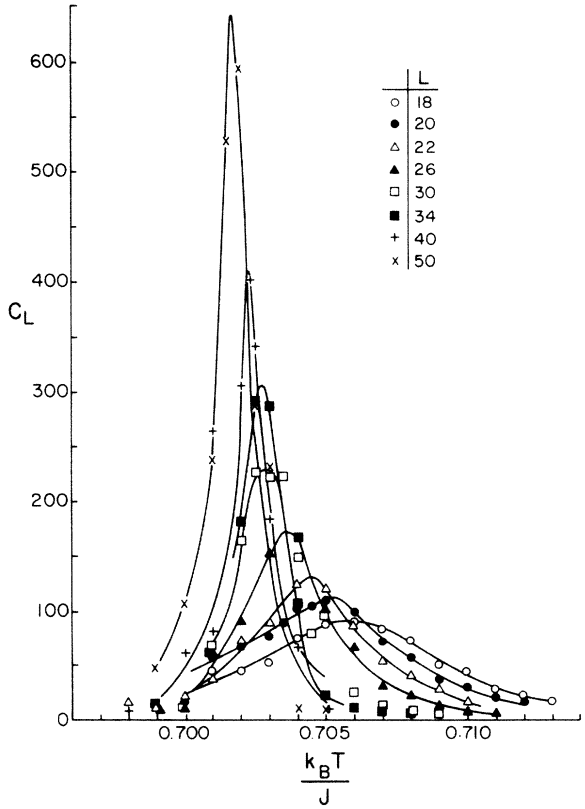

FIG. 5. Temperature variation of the specific heat for various lattice sizes. Data for some lattice sizes have been omitted in order to preserve the clarity of the figure.

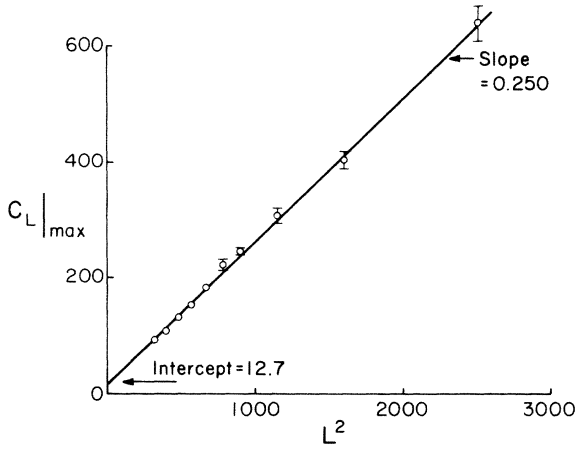

FIG. 6. Variation of the specific-heat maxima with L^d.

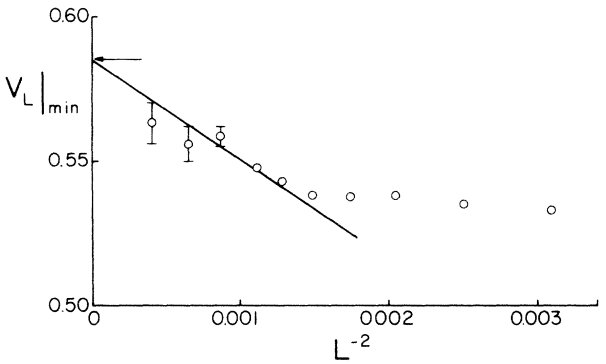

FIG. 8. Variation of $V_L|_{min}$ with L^{-d}. The arrow shows the infinite lattice value obtained from Eq. (28a).

were performed on the CDC Cyber 205 vector processor at the University of Georgia. Using a memory-to-register swapping technique suggested by Wansleben *et al.*[24] and a newly-developed "checkerboard" algorithm (for background see Ref. 25) we obtained a speed of 1.6 μsec per update. The speed on the vector processor was about 35 times the speed we obtained on the Cyber 750, a fast scalar machine. The advantage of a super computer is obvious: the equivalent CPU time on the Cyber 750 would have been enormous.

The temperature variation of the specific heat for various lattice sizes is shown in Fig. 5. As the lattice size increases, the peaks grow while the rounding decreases. The rounding is already very small for $L=18$ (half-width, $\Delta T_{1/2} \approx 0.0077$). There is also a definite shift in T_L^C. The peak heights are plotted versus volume in Fig. 6 and we see an excellent straight-line behavior in accordance with Eq. (23). A least-squares fit yields a slope of 0.250—within 1.6% of the theoretical value. There are no theoretical values for the intercept and we estimate $C_+ + C_- = 25.4$ from the fit. This should be good enough for a rough estimate.

The temperature variation of V_L is shown for various lattice sizes in Fig. 7 and confirms our expectations. There is a prominent minimum even for $L=50$ and definite L dependence in T_L^V. We present in Fig. 8 the variation of $V_L|_{min}$ with L^{-d} [Eqs. (28a) and (28b)]. $V_L|_{min}$ does increase for the larger lattices though the data becomes increasingly inaccurate. The straight line is the best-fit line passing through the limiting value and the data for the larger lattices after taking into account the error bars. However, this extrapolation is questionable because the slope is larger than the theoretical value [see Eq. (28b)] by a factor of 4. On one hand it is possible that the theory is in serious error because the Gaussian approximation, being completely determined by the first and second moments, gives wrong numerical values for the fourth moment. (A more realistic theory would, for example, account for the variation of C_+ and C_- with temperature.

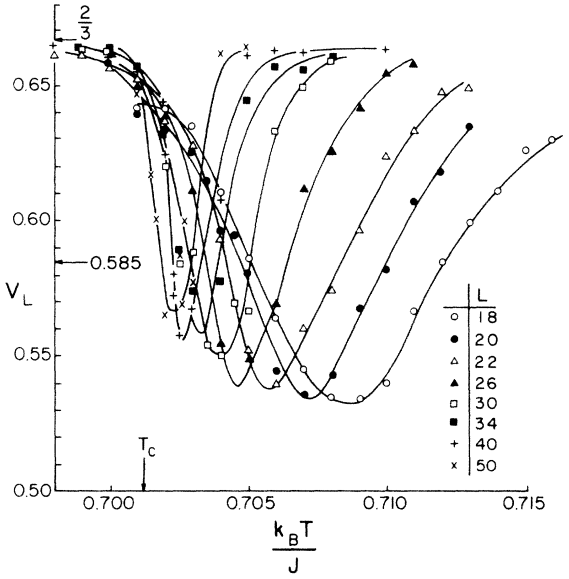

FIG. 7. Temperature variation of V_L for various lattice sizes. The transition temperature and the trivial ($\frac{2}{3}$) and nontrivial (0.585) limits for $V_L|_{min}$ are indicated. Data for some of the lattice sizes have been omitted in order to preserve the clarity of the figure.

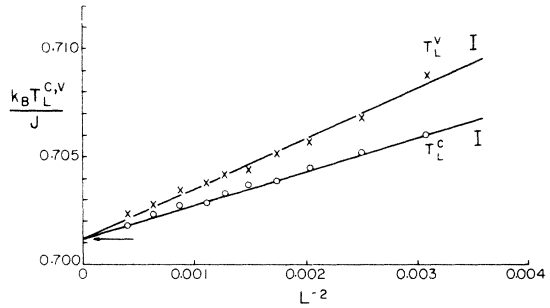

FIG. 9. Extrapolation of the characteristic temperatures versus L^{-d}. T_L^C is the location of $C_L|_{max}$ and T_L^V is the location of $V_L|_{min}$. The arrow shows the infinite lattice value obtained from Eq. (30). The maximum error bars are also indicated.

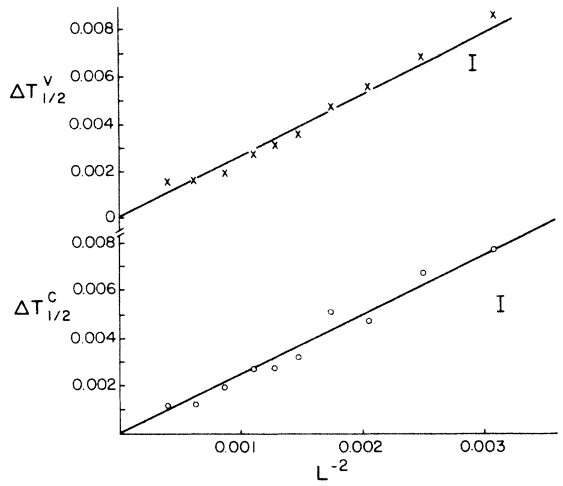

FIG. 10. Extrapolation of the rounding "fields" versus L^{-d}. The $\Delta T^{c}_{1/2}$ are the half-widths of the specific-heat maxima in Fig. 5 and the $\Delta T^{v}_{1/2}$ are the half-widths of the V_L minima in Fig. 7. The maximum error bars are also indicated.

Note that this would only affect the approach to the limit and not the limit itself.) On the other hand, the errors in V_L for $L=40$ and 50 prevent us from ascertaining the asymptotic behavior. Thus, while we are satisfied with the qualitative behavior of V_L, we are at present unable to say more on the quantitative aspects.

In Fig. 9 we present the variation of $T_L^{C,V}$ with L^{-d} in accordance with Eq. (18). There is excellent linear behavior and T_c thus found agrees with the theoretical result to four significant figures.

Figure 10 presents the variation of the rounding with L^{-d}. While there is some scatter in the data most of it is due to errors in drawing the curves of Figs. 5 and 7. The slopes of the straight lines (≈ 2.5) are in rough agreement with the order of magnitude estimate (≈ 1.4) of Eq. (20).

We see from Eq. (9) that if $C_+ = C_-$ we would have a nice scaling form: C_L/L^d would be a universal function of $\Delta T L^d$. There would be small corrections due to the first term in Eq. (9) but we expect these corrections to be quite small for the lattice sizes in our work. We expect that $E_+ - E_-$ and $C_+ - C_-$ would be of order unity and since we are interested in ΔT of order L^{-d}, the term $\Delta T(C_+ - C_-)$ in the numerator of Eq. (9) is only another small correction to scaling. Scaling was attempted, using $\Delta T = T - T_L^C$ and the results are shown in Fig. 11(a). The scatter in the data is due to problems in sampling the distributions (even with $> 10^7$ MCS/site) and we conclude that scaling works reasonably well. Note that sampling the distribution functions accurately is enormously difficult: Most of the time the system stays close to one of the peaks, but to get the relative weight of the peaks correctly one has to pass from one peak to the other very often, going through the deep minimum separating them in the process. In fact, with runs employing the ordinary statistical effort of a few thousand MCS/site, one would observe hysteresis and would not be able to meaningfully sample the distribution $P_L(E)$ at all.

The theoretical analysis of Sec. II implies that C_L/L^2

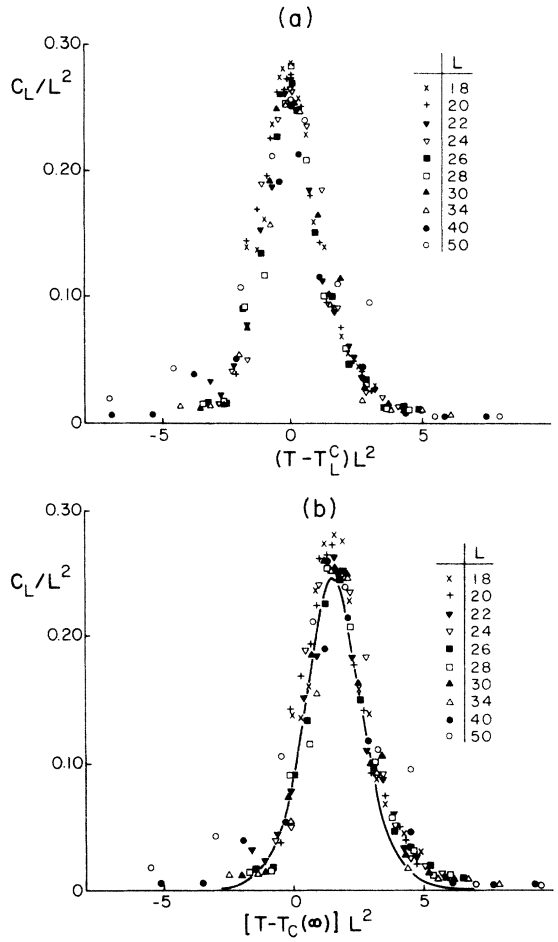

FIG. 11. Scaling of the specific-heat data. (a) T_L^C in the abscissa is the location of the specific-heat maximum for a lattice of size $L \times L$. (b) $T_c(\infty)$ in the abscissa is the transition temperature of the infinite lattice. The solid curve results from Eq. (35).

should also be a scaled function of $(T-T_c)L^d$, where $T_c = T_\infty^c$ is the infinite system critical temperature rather than the shifted critical temperature as employed in Fig. 11(a). This full scaling description is tested in Fig. 11(b); the shift of T_c in the finite system now shows up as a displacement of the peak from the origin to $(T-T_c)L^2 \approx 1.5$. We see that the data again scale reasonably well, and moreover, are described by the scaling function which follows from Eq. (9)

$$\frac{C_L}{L^2} = \frac{(E_+ - E_-)^2 q (C_-/C_+)^{1/2}}{k_B T_c^2 [e^x + e^{-x} q (C_-/C_+)^{1/2}]^2}, \tag{35}$$

which is included in Fig. 11(b) by choosing $C_-/C_+ = 0.70$. The systematic deviations at the peak should be attributed to the additive correction term in Eq. (9), while the systematic deviations far out in the wings are partly due to the term $(C_+ - C_-)\Delta T$ in Eq. (9) which also represents a correction to scaling. Note that apart from the ratio C_-/C_+ which also can be extracted from the data in Fig. 9 by applying Eq. (18), all other parameters in the above scaling function are known exactly and

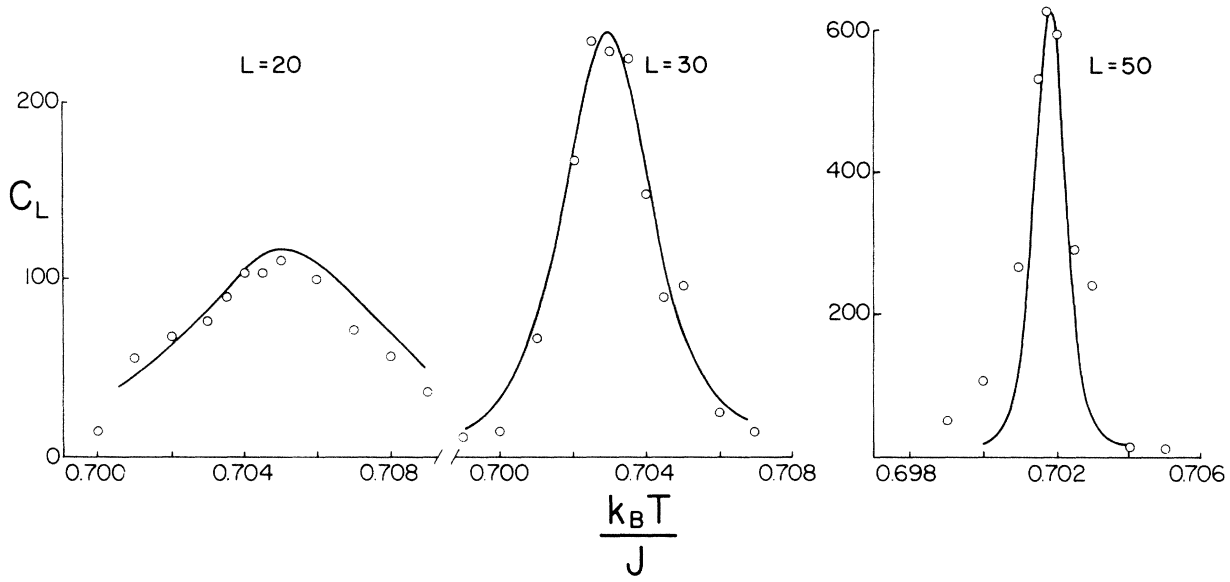

FIG. 12. Specific heat for three $L \times L$ lattices plotted versus temperature. Open circles are the Monte Carlo results while the solid curves represent Eq. (9) for $C_-/C_+ = 0.7$ (the other parameters being taken from the exact solution, see Table I).

are not adjustable. Thus the agreement between this function and the Monte Carlo data confirms the basic assumptions of our theoretical analysis. In Fig. 12 we show the comparison between the specific-heat data for three different lattice sizes and Eq. (9) which includes the lowest-order corrections to the simplest scaling form using $C_-/C_+ = 0.7$. The agreement is quite reasonable but the statistical fluctuations in the data make it impossible to accurately extract further corrections. We also find that comparatively good fits are obtained for other choices of C_-/C_+ in the range between $C_-/C_+ = 0.5$ to $C_-/C_+ = 0.9$. Combining our "best estimate" $C_-/C_+ = 0.7$ with the result for $C_+ + C_-$ as obtained from the extrapolation in Fig. 6, we obtain rough estimates for C_+ and C_- individually as shown in Table I.[26]

We remarked earlier [Eqs. (23)—(28)] that the fourth-order quantity, V_L, has a characteristic behavior at a first-order transition. This may be contrasted with the behavior of V_L at a second-order transition. Since the order of the transition in the Potts model is q dependent, it was a simple matter to change the program in order to study V_L at second-order transitions. The results are shown in Fig. 13 for $q = 2$ and 3. We see that our expectations are borne out well. (The minimum in V_L at a second-order transition is due to the specific-heat maximum which diverges as $L^{\alpha/\nu}$. However, this is smaller than L^d and the minimum disappears rapidly with increasing lattice size.)

Once the transition temperature is located accurately from extrapolations such as those shown in Fig. 9, estimates for E_+ and E_- may be obtained by making short runs at the transition temperature on a very large lattice.

TABLE I. Thermodynamic quantities obtained from simulations on a 500×500 lattice using 10 000 MCS. The results are compared with the known values for the infinite lattice.

Quantity	From simulations on a 500×500 lattice	From present extrapolations	Exact results
$k_B T_c/J$		0.7012±0.0001	0.701 232...
E_-/J	1.6661±0.0043	1.64±0.02[a]	1.6643...[b]
E_+/J	−0.9716±0.0027	0.94±0.02[a]	−0.9682...[b]
C_-	14±6	10.5±2.0	
C_+	15±6	14.9±2.0	
$C_+ + C_-$	29±8	25.4±0.2[c]	
M_-	0.8587±0.0032		0.8575[d]
M_+	0.0071±0.0023[e]		0

[a] $E_- - E_-$ follows from the slope of Fig. 6, while $E_+ + E_-$ follows from $\langle E \rangle_L$ at T_c^L, see Eq. (16).
[b] From Eqs. (31) and (32).
[c] From Fig. 6. Note that $C_+ + C_-$ can hence be estimated more accurately than C_+, C_- individually.
[d] From Eq. (34).
[e] The order parameter cannot vanish in a finite system.

This ensures that the system stays within one state during the run, and one can use the quantities thus obtained as a cross check. This procedure is particularly valuable in cases where no exact solution is available. This has been done on a 500×500 lattice using 10000 MCS and the results are shown in Table I. There is very good agreement between the energy and magnetization values but only a rough agreement with the specific-heat values. This is not surprising since the specific heat is very large and, hence, sampling it very accurately, using short runs, is very difficult.

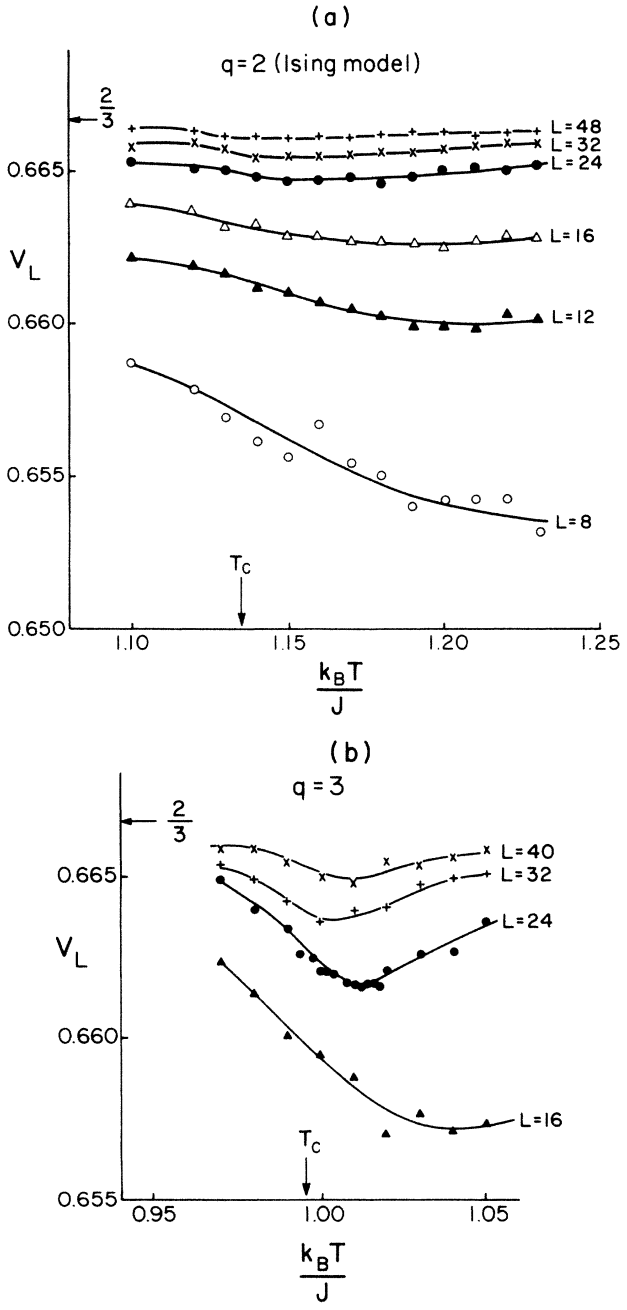

FIG. 13. Temperature variation of V_L for various lattice sizes at second-order transitions. (a) Data for the $q=2$ Potts model using 30000 MCS. The transition temperature shown is obtained from Eq. (30). The exchange constant, J, is twice that of the Ising model. (b) Same as (a) for the $q=3$ Potts model.

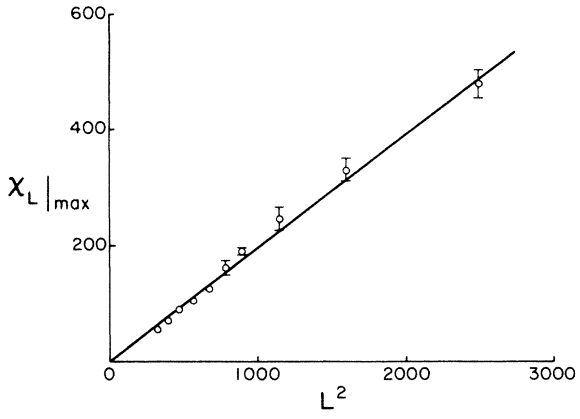

FIG. 14. Variation of the susceptibility maxima with volume in the ten-state Potts model.

The purpose of the present work has been to study the moments of the energy distribution, and the moments of the magnetization distribution have been omitted from the discussion so far. One of the reasons is that the quantity, U_L, which may be defined in a manner analogous to V_L, has its minimum far away from T_L^V and it was not possible to study it in equal depth. Another reason is that the magnetization distribution has been analyzed in detail in I and the only changes appropriate here would be that the widths of the distribution will depend on the "susceptibilities" instead of the specific heats. Care is needed if one studies order-parameter variation with *temperature* and not field since "mixed susceptibilities" such as $dm/dT \propto \langle mE\rangle - \langle m\rangle\langle E\rangle$, also enter. The characteristic features will not differ; for example, the susceptibility does diverge as L^d (Fig. 14) and the locations of the susceptibility maxima vary as L^{-d} (Fig. 15). For purposes of illustration, we present in Fig. 16 the temperature variation of the fourth-order cumulant of the order parameter: $U_L = 1-\langle m^4\rangle_L/3\langle m^2\rangle_L^2$ (not to be confused with the internal energy).

IV. CONCLUSIONS

The phenomenological theory we have presented predicts that all finite-size effects depend on the volume

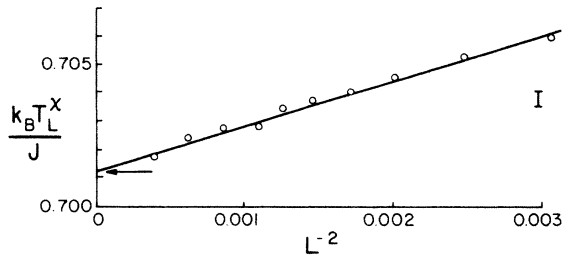

FIG. 15. Extrapolation of the location of the susceptibility maxima in the ten-state Potts model. The maximum error bars are indicated.

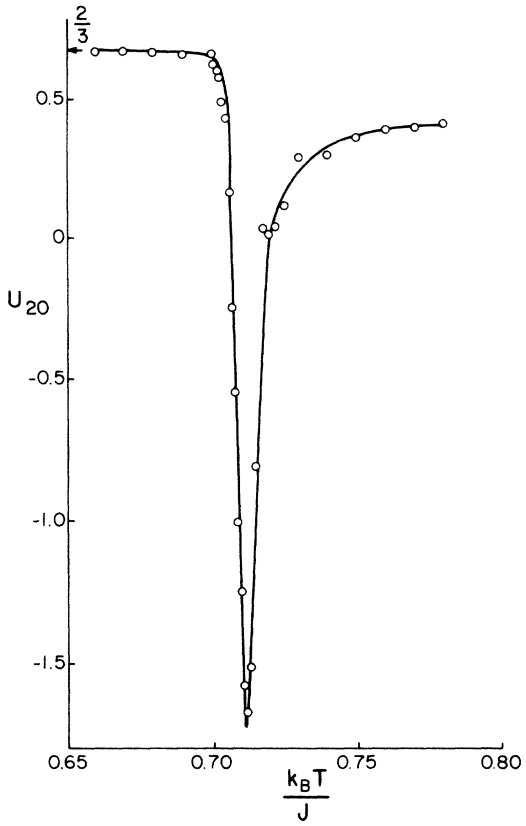

FIG. 16. Temperature variation of the fourth-order quantity U_L for $L=20$ in the ten-state Potts model. U_L is the magnetization analog of V_L. Note that the temperature scale is 10 times smaller than that used in Fig. 7.

L^d. This is consistent with other approaches and with the results of our simulations. The numerical predictions regarding the specific heat are in very good agreement with the results from simulations. The fourth-order quantity, V_L, has proved useful in clarifying the nature of the transition (however, the theory does not yield reliable numerical values for the explicit L dependence of V_L). We have therefore demonstrated that the present analysis of size effects at a temperature-driven transition can identify its order and that we can obtain the various quantities of interest in a well-controlled manner. Note that this is a nontrivial result—standard Monte Carlo simulations of two-dimensional Potts models using only one moderately large lattice size ($L=60$) and moderate statistics[27] *could not* distinguish whether the transition for $q=5$ and for $q>6$ state Potts models is first or higher order. This approach is particularly useful for the study of models where the order parameter is not known and, e.g., for lattice gauge models for which it is believed that no order parameter exists. Similarly in studies of systems with continuous spatial symmetry, e.g., Lennard-Jones liquid-gas and liquid-solid transition models, this approach should also be useful.

ACKNOWLEDGMENTS

We are thankful for the programming assistance of Dr. David Matthews-Morgan of the Advanced Computational Methods Center at the University of Georgia. This research was supported in part by the National Science Foundation under Grant No. DMR-8300754.

*Permanent address.
[1]M. E. Fisher, in *Critical Phenomena,* edited by M. S. Green (Academic, New York, 1971).
[2]A. E. Ferdinand and M. E. Fisher, Phys. Rev. **185**, B832 (1969).
[3]M. E. Fisher and M. N. Barber, Phys. Rev. Lett. **28**, 1516 (1972).
[4]M. P. Nightingale, Physica **83A**, 561 (1976).
[5]D. P. Landau, Phys. Rev. B **13**, 2997 (1976); **14**, 225 (1976).
[6]K. Binder, Phys. Rev. Lett. **47**, 693 (1981); Z. Phys. B **43**, 119 (1981).
[7]For a recent review of finite-size scaling see M. N. Barber, in *Phase Transitions and Critical Phenomena,* edited by C. Domb and J. L. Lebowitz (Academic, New York, 1983), Vol. 8, p. 145; see also K. Binder, *ibid.*, Vol. 8, p. 1.
[8]Y. Imry, Phys. Rev. B **21**, 2042 (1980).
[9]M. E. Fisher and A. N. Berker, Phys. Rev. B **26**, 2507 (1982).
[10]J. L. Cardy and M. P. Nightingale, Phys. Rev. B **27**, 4256 (1983).
[11]V. Privman and M. E. Fisher, J. Stat. Phys. **33**, 385 (1983).
[12]K. Binder and D. P. Landau, Phys. Rev. B **30**, 1477 (1984).
[13]V. Privman and M. E. Fisher, J. Appl. Phys. **57**, 3327 (1985).
[14]A complete treatment of thermodynamic fluctuations can be found in Landau and Lifshitz, *Statistical Physics,* Vol 5 of *Course of Theoretical Physics* (Pergamon, New York, 1980), part I.
[15]This may be justified by appealing to the central limit theorem. See, for example, L. E. Reichl, *A Modern Course in Statistical Physics* (Univesity of Texas Press, Austin, 1980).
[16]K. Binder and D. Stauffer, Adv. Phys. **25**, 343 (1976); J. D. Gunton *et al.*, in *Phase Transitions and Critical Phenomena,* edited by C. Domb and J. L. Lebowitz (Academic, New York, 1983), Vol. 8.
[17]V_L as defined here is slightly different from U_L defined in Ref. 12. The quantity is a sort of reduced cumulant.
[18]See, for example, K. Binder, in *Monte Carlo Methods in Statistical Physics,* edited by K. Binder (Springer, Berlin, 1979).
[19]For a review on the Potts model, see F. Y. Wu, Rev. Mod. Phys. **54**, 235 (1982).
[20]R. J. Baxter, J. Phys. C **6**, L445 (1973).
[21]T. Kihara, Y. Midzuno, and T. Shizume, J. Phys. Soc. Jpn. **9**, 681 (1954).
[22]D. Kim, Phys. Lett. **87A**, 127 (1981).
[23]R. J. Baxter, J. Phys. A **15**, 3329 (1982).
[24]S. Wansleben, J. G. Zabolitsky, and C. Kalle, J. Stat. Phys. **37**, 271 (1984).
[25]W. Oed, Appl. Informatics **7**, 358 (1982).
[26]$C_+ - C_-$ may be obtained from the exact results of either Ref. 20 or Ref. 21. We find $C_+ - C_- = (E_+ - E_-)/T_c^2\sqrt{q} = 0.4477$. While the best estimates obtained from the simulations (Table I) are larger than this, the values agree to within the error bars.
[27]K. Binder, J. Stat. Phys. **24**, 51 (1981).